Investigation on Structural Behaviour of Composite Cold-Formed Steel and Reinforced Concrete Flooring Systems

Omar A. Shamayleh*[1], Harry Far[1a]

[1] *School of Civil and Environmental Engineering, Faculty of Engineering and Information Technology, University of Technology Sydney (UTS), Sydney, Australia*

(Received keep as blank , Revised keep as blank , Accepted keep as blank)

Abstract. Composite flooring systems consisting of cold-formed steel joists and reinforced concrete slabs offer an efficient, lightweight solution. However, utilisation of composite action to achieve enhanced strength and economical design has been limited. In this study, finite element modelling was utilised to create a three-dimensional model which was then validated against experimental results for a composite flooring system consisting of cold-formed steel joists, reinforced concrete slab and steel bolt shear connectors. This validated numerical model was then utilised to perform parametric studies on the performance of the structural system. The results from the parametric study demonstrate that increased thickness of the concrete slab and increased thickness of the cold formed steel beam resulted in higher moment capacity and stiffness of the composite flooring system. In addition, reducing the spacing of bolts and spacing of the cold formed steel beams both resulted in enhanced load capacity of the composite system. Increasing the concrete grade was also found to increase the moment capacity of the composite flooring system. Overall, the results show that an efficient, lightweight composite flooring system can be achieved and optimised by selecting suitable concrete slab thickness, cold formed beam thickness, bolt spacing, cold formed beam spacing and concrete grade.

Keywords: Composite Cold-Formed Steel and Reinforced Concrete Flooring Systems, Cold-Formed Steel Beams, Composite Floors, Finite Element Method, Composite Action, Flexural Behaviour.

1. Introduction

The use of cold-formed steel as load-bearing and non-load bearing members has been widely adopted in the construction industry (Kyvelou 2017; Malite et al. 1998). However, research has shown that significant economic benefits can be achieved by using composite cold-formed steel and reinforced concrete beams and flooring systems, resulting in superior properties to typical reinforced concrete-hot rolled steel composite systems (Abdel-Sayed 1982). In addition to being inherently light-weight, cold-formed steel composite structures allow for flooring systems with relatively shallow depth, which can in turn result in lower overall building height (Ahmed & Tsavdaridis 2019). Further, such systems can be effectively adjusted to irregular geometries providing further economic benefits and allowing for flexibility in the architectural design (Ahmed & Tsavdaridis 2019; Paton-Cole & Gad 2017).

Additionally, the manufacturing processes for cold formed steel —press-braking or roll-forming —are relatively simple compared to hot rolled steel, which require large plants with significant investment (Yu, LaBoube & Chen 2020). Cold formed steel (CFS) sections can be readily modified to produce built-up sections with relative ease compared to hot-rolled steel, facilitating rapid construction.

*Corresponding author, Ph.D. Student
E-mail: Omar.A.Shamayleh@student.uts.edu.au
[a]Ph.D.

This makes composite cold-formed construction feasible, especially for small to medium projects and in less developed countries and remote regions where hot-rolled steel sections are not readily available (Framecad 2018; Hanaor 2000). Fig. 1 shows an example of a building in the United States featuring a flooring system with cold formed steel beams.

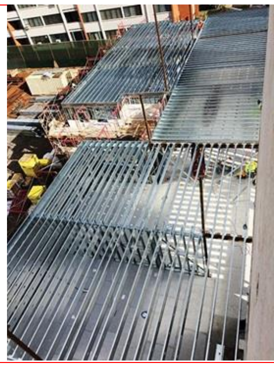

Fig. 1 Example of a flooring system utilising cold-formed steel beams (Wills 2015)

Research has shown that significant economic benefits can be achieved by using composite cold-formed steel and reinforced concrete beams and flooring systems (Abdel-Sayed 1982). This trend has manifested in increased demand for lightweight construction, with an expectation of nearly 5% annual growth in the global light gauge steel framing market over the next few years (Grand View Research 2021).

However, composite reinforced concrete and cold-formed steel sections have had limited use to date (Bamaga et al. 2013), due in part to the lack of provisions in existing building codes for such systems (Hanaor 2000; Wehbe et al. 2011). Current standards and specifications, including Australian standards such as AS/NZS 2327:2017, to date provide very limited guidance related to the design of composite structures incorporating built-up cold-formed steel members (Standards Australia 2017). Thus, research is required to expand the scope of these standards to allow for composite steel-concrete construction using a variety of cold formed steel members and configurations (Rasmussen et al. 2020).

Various, innovative composite systems utilising cold formed steel and reinforced concrete have been proposed. Abdel-Sayed (1982) conducted experiments to determine the structural behaviour of concrete beams, with traditional rebar replaced by a cold-formed channel section. This idea was further developed and tested by Nguyen (1991), who studied the possibility of reducing the construction cost associated with formwork and shoring by replacing conventional rebar with an a cold formed steel, lipped-channel section of equivalent cross sectional area. Researchers have found that dedicated shear connectors create an efficient bond between the different components of a composite flooring system (Bamaga et al. 2019; Kyvelou 2017; Nakamura 2002). Unlike composite reinforced concrete-hot rolled steel systems, welding shear studs to cold-formed steel sections is impractical due to the thin nature of cold-formed steel sections (Hanaor 2000).

Wehbe et al. (2011) explored the feasibility of a composite beam system comprising reinforced concrete and a cold-formed steel track, which functions as the steel reinforcement, with composite action being provided by standoff screws. The authors reported that the composite sections could be designed for ductile flexural failure, provided that an adequate number of screws were provided. A minimum density of 2 screws every 150mm was found to be required to prevent relative slip between the concrete and cold-formed steel track and mobilise the composite action, in which case the response of the composite beam could be determined with accuracy.

Nakamura (2002) proposed a composite bridge girder system with steel, U-shaped girders fabricated from a single steel sheet. Shear studs provided a connection between the U-shaped cold-formed section and the reinforced concrete slab. Nakamura (2002) found that these sections achieved composite behaviour, observing experimentally that the cold formed steel U-section and concrete slab "worked together as one piece until the yield point" (Nakamura 2002). Based on the findings of their experimental investigation, Nakamura (2002) proposed a design method based on plastic design principals.

These results were confirmed by Hanaor (2000), who tested a variety of configurations of cold formed steel-reinforced concrete composite sections, in addition to conducting push-out tests of several varieties of shear connectors including self-drilling screws and a welded shear connector. The authors found the response of the cold-formed composite beams to be highly ductile, indicating the success of the shear connections in ensuring composite action and affirming the viability of such systems. Hanaor (2000) further deduced that design codes incorporating provisions for the design of composite structures such as BS 5400: Pt. 5 (BSI 2005 and earlier editions), a British design standard for composite bridges, conservatively determined the capacity of connectors, such that further investigations and updating of codes could enable better utilisation of cold-formed steel-reinforced concrete composite sections.

Subsequent researchers proposed various types of shear connectors. An alternate shear transfer mechanism was studied by Lakkavalli & Liu (2006) and Irwan et al. (2011), in the form of bent-up shear tabs. This mechanism proved to be effective, such that the end-bearing against the cross section of the tabs provided resistance to longitudinal shear, successfully ensuring composite action of the proposed section.

The research summarised above provided valuable insight into the behaviour of composite cold-formed steel and reinforced concrete flooring systems. However, experimental investigations alone are insufficient to examine all the factors influencing the response of such systems, particularly due to time and cost considerations (Karki, Far & Saleh 2021). Thus the need emerges for a numerical model capable of accurately modelling the proposed composite flooring system and producing results which are closely similar to those achieved by experimental investigations (Alhajri et al. 2016). Achieving such a model will allow for a broad investigation of such systems and for expanding the findings. Consequently, the current study presents a numerical investigation into the parameters which dictate the behaviour of the proposed cold formed steel - reinforced concrete composite flooring system, including the variations of the thickness of the concrete slab, the thickness of the cold formed steel joist and the spacing of the bolted shear connectors. Results from four-point bending tests carried out by Alhajri et al. (2016) have been utilised to validate the numerical model.

2. Finite Element Modelling

The significance of nonlinear finite element modelling to establish and investigate the behaviour of composite cold formed steel flooring systems has been established by numerous researchers, with numerical results typically achieving high accuracy in comparison with experimental results (Alhajri et al. 2016; Far 2020; Karki, Far & Saleh 2021; Kyvelou, Gardner & Nethercot 2018). In the current study, ANSYS 2021 R2 (ANSYS Inc. 2021) was used to conduct the numerical investigation. Material properties and test data were obtained from Alhajri et al. (2016). The physical testing was carried out on an I-section beam consisting of two back-to-back C-channels, the top flanges of which were attached to the reinforced concrete slab as shown in Fig. 3. However, in the current study, computational efficiency was achieved by modelling a quarter of experimental setup, applying the correct boundary conditions on two axes of symmetry. This allowed for significant reduction in computational time. Validation of the experimental results detailed in Alhajri et al. (2016) was conducted utilising this finite element model. The validated model was subsequently used to conduct parametric studies investigating the influence of thickness of concrete slab, thickness of the cold-formed steel beam, spacing between beams, spacing of bolts and concrete grade on the structural behaviour of the composite flooring system.

2.1 Properties of Materials

The composite beam under investigation consists of a cold formed steel (CFS) beam, reinforced concrete slab and bolts. Material properties used in the current study have been adopted from (Alhajri et al. 2016), wherein compressive strength testing of concrete was conducted as per ASTM standards. For the CFS beam, yield and ultimate strength were obtained by cutting coupon tensile test specimens from the web and flange of the CFS C-section. As per Alhajri et al. (2016), high strength bolts of grade 8.8 were used. Table 1 summarises the mechanical properties of the cold formed steel used in this study, and the curve for strain hardening behaviour is given in Fig. 2.

Table 1 Average measured mechanical properties of cold-formed steel

Material Characteristics	Value
Modulus of elasticity, E (MPa)	198000
Poisson's ratio, υ	0.3
Yield strength, (MPa)	329
Tensile strength, σu (MPa)	427
Tangent Modulus (MPa)	11950

Source: Adapted from Alhajri et al. (2016)

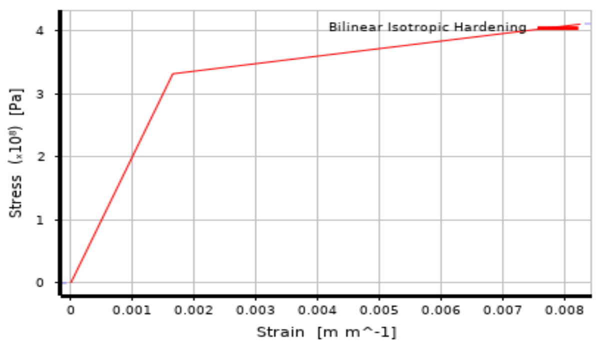

Fig. 2 Bilinear stress-strain curve for cold-formed steel
Source: Adapted from Alhajri et al. (2016)

The compressive strength (cube) of the mortar used in this study is 35 MPa. The mechanical properties of the mortar, including compressive strength fcu and modulus of elasticity, E were obtained by Alhajri et al. (2016) through cube compression tests and adopted in the current study. The mechanical properties of the mortar are summarised in Table 2. The mechanical properties of these bolts were obtained from Alhajri et al. (2016) and are summarised in Table 3.

Table 2 Average measured mechanical properties of concrete

Material Characteristics	Value
Modulus of elasticity, E (MPa)	26200
Poisson's ratio, υ	0.2
Compressive strength, (MPa)	35

Source: Adapted from Alhajri et al. (2016)

Table 3 Average measured mechanical properties of steel bolt

Material Characteristics	Value
Modulus of elasticity, E (MPa)	202000
Poisson's ratio, υ	0.3
Yield strength, (MPa)	704
Tensile strength, σu (MPa)	906

Source: Adapted from Alhajri et al. (2016)

2.2 Numerical Study Procedure

The finite element software ANSYS (ANSYS Inc. 2021) was utilised in this study to simulate the response and behaviour of the composite cold-formed steel – reinforced concrete beam, using a three dimensional finite element model. Previous studies have shown that 3D models give higher accuracy for results compared to two-dimensional models (Alhajri et al. 2016; Far 2020; Kyvelou, Gardner & Nethercot 2018).

The cold-formed steel beam was modelled using SHELL 181 element, which is a four-node element with each node having six degrees of freedom; translation and rotation about the x, y and z-axes. SOLID 186 was used for modelling the concrete slab. SOLID 186 is a 3D element, featuring twenty nodes each with three degrees of freedom, translation in the x, y and z-axes. This type of element supports a range of mechanical properties including plasticity, creep, large deflection, and large strain capabilities, making it a versatile modelling tool.

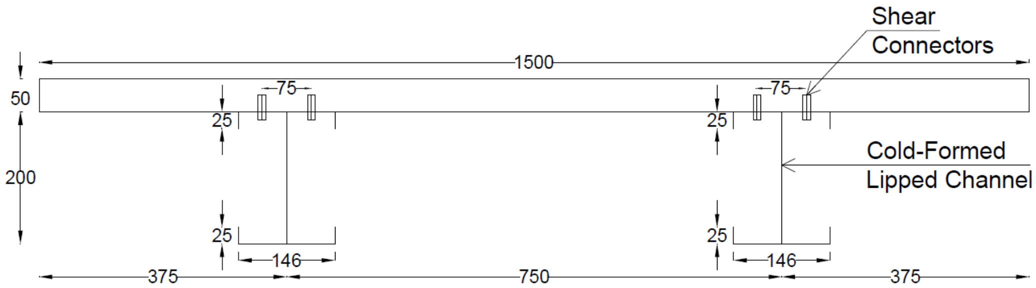

Fig. 3 Cross-section of composite beam (Alhajri et al. 2016)

The contact between the reinforced concrete slab and the top flange of the cold formed steel beam was modelled using the CONTA174 element, using a friction coefficient of 0.3 (Karki, Far & Saleh 2021). The bolts that serve as the shear connection between the cold-formed steel beam and concrete slab were modelled using the COMBIN39 element. COMBIN39 is a unidirectional nonlinear spring element with nonlinear generalised force-deflection capabilities. The element is defined by two node points and a generalized force-deformation curve (Mantha 2014). The load-slip response of bolts shown in Fig. 4, which were experimentally calculated by Hosseinpour et al. (2021), was utilised in this numerical investigation for the spring behaviour of COMBIN39 element.

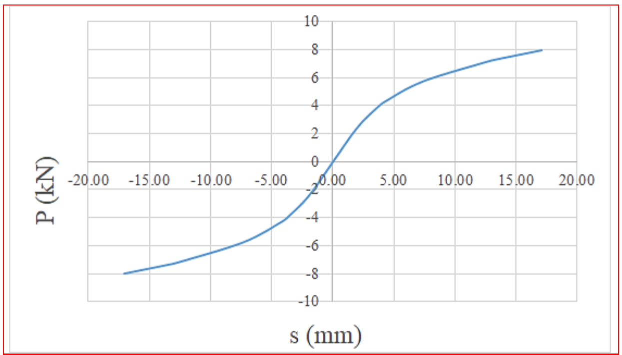

Fig. 4 Load the load-slip relationship of the shear connectors used in the numerical model

The element size for the 3D elements used in the reinforced concrete slab was 50mm × 50mm ×13mm, while for the CFS beam the element size was 50mm × 6mm × 3mm. The finite element mesh for the composite beam finite element model is shown Fig. 5.

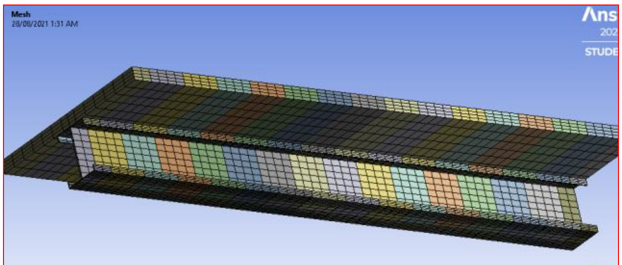

Fig. 5 Overview of the model geometry

In order to determine the suitability of the mesh size, a mesh sensitivity analysis was carried out as shown in Fig. 6. The results show minimal improvement in the accuracy of results when utilising a 30×30mm element size, when compared to the adopted 50×50mm element size and experimental results from Alhajri et al. (2016), at the expense of considerably increased analysis time. Using a larger element (70×70mm) yielded a value of ultimate load and maximum deflection considerably higher than the experimental results from Alhajri et al. (2016); 4.29% and 13.59%, respectively. These results confirm the selection of 50×50mm element size as suitable in terms of accuracy of results and efficiency of computational time.

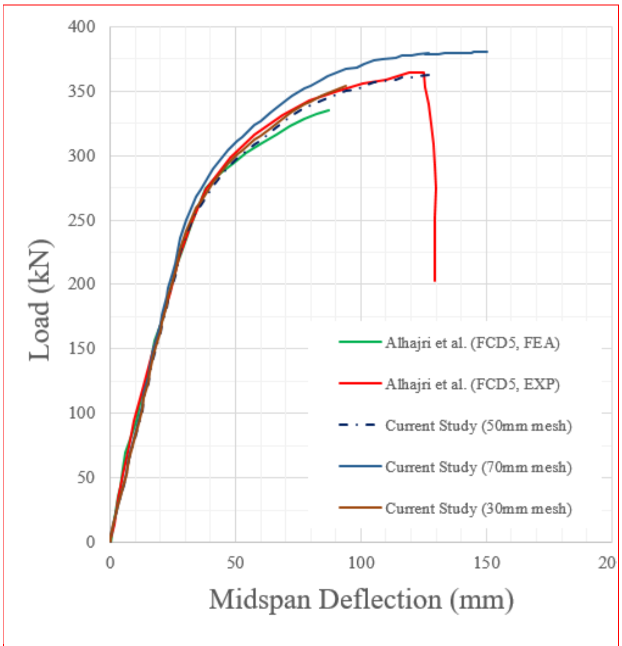

Fig. 6 Comparison of Load-deflection responses of Specimen FCD5 using various mesh sizes

The composite beam implemented in this study is 4500mm long with a span of 4200mm between supports. The width of the reinforced concrete slab was 1500mm, and the thickness was 50mm. The cold formed steel beams consist of two lipped C-channels placed back-to-back, such that the reinforced concrete slab is attached to the top flange, and incorporating bolts as shear connectors. A simplified sketch showing the arrangement of the four-point bending test and composite beam is shown in Fig. 7. To simplify the analysis and reduce computational cost, symmetry was considered in two directions as shown in Fig. 8.

3. Validation of Finite Element Models

In order to gauge the accuracy of the numerical model constructed for the purposes of this study, the results of the numerical simulations were compared to results in the literature for the purpose of validation. Namely, results were validated against experimental and numerical results obtained by Alhajri et al. (2016).

Subsequently, the validated model was utilised in parametric studies to examine the effect of thickness of concrete slab, thickness of the cold-formed steel beam, spacing between beams, spacing of bolts and concrete grade. Only one of these parameters was varied at time, keeping the cross-sectional shape constant in order to examine the effect of each of these parameters. Alhajri et al. (2016) tested nine composite beam specimens comprising a concrete slab and CFS beam with differing thickness of CFS beam. Out of these nine flooring systems, two were used to validate the Finite Element Models developed in the current investigation. Specimen FCD5 with 3mm thick CFS, and specimen FCD8 with 4mm thick CFS were selected, as shown in Table 4.

Table 4 Summary of systems tested (adopted from Alhajri et al. (2016)) for validation of numerical model

Specimen	FCD5	FCD8
CFS beam thickness (mm)	3	4
Bolt spacing (mm)	150	150
Thickness of reinforced concrete slab (mm)	50	50

Source: Adapted from Alhajri et al. (2016)

The typical failure mode of the specimen FCD5 (Alhajri et al. 2016) was found to comparable to the failure mode observed in the numerical investigation conducted in the current study. Namely, distortional buckling was observed in the bottom flange of the CFS beam as shown in Fig. 9a. Additionally, the load deflection response of the specimen FCD5 (Alhajri et al. 2016) was found to be similar to the current study, as shown in Fig. 9b.

The load deflection response of the specimens FCD5 and FCD8 were found to be closely compatible with the current study, as shown in Fig. 10 and Fig. 11, respectively.

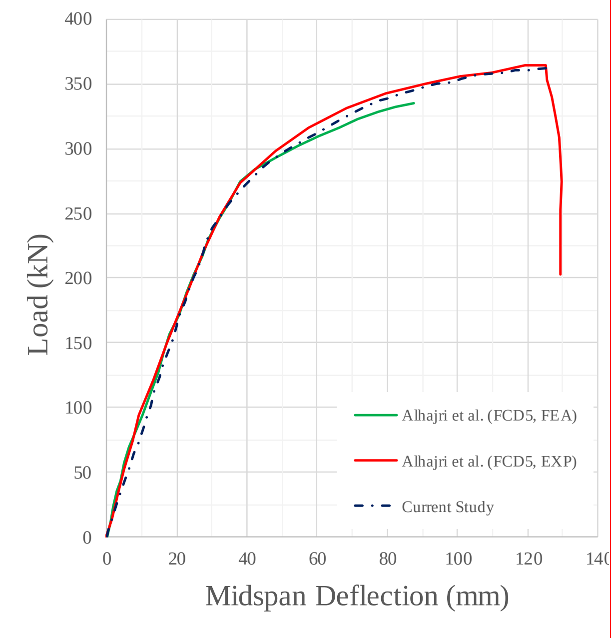

Fig. 10 Comparison of Load-deflection responses of Specimen FCD5.

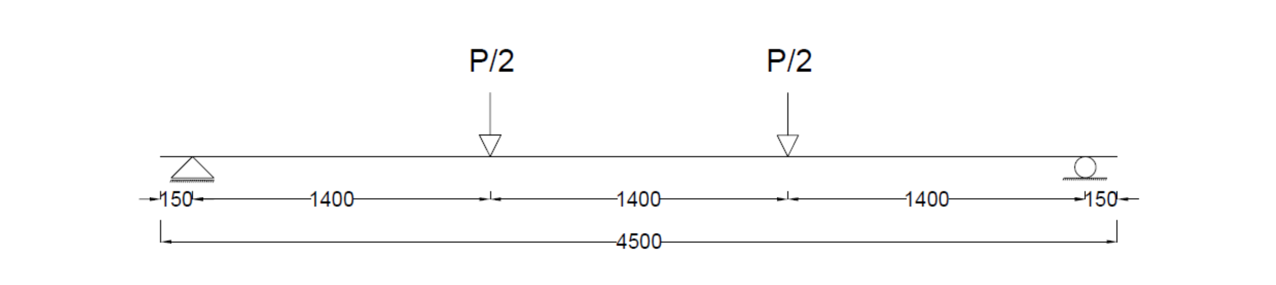

Fig. 7 Simplified sketch of the four point bending test considered in this study

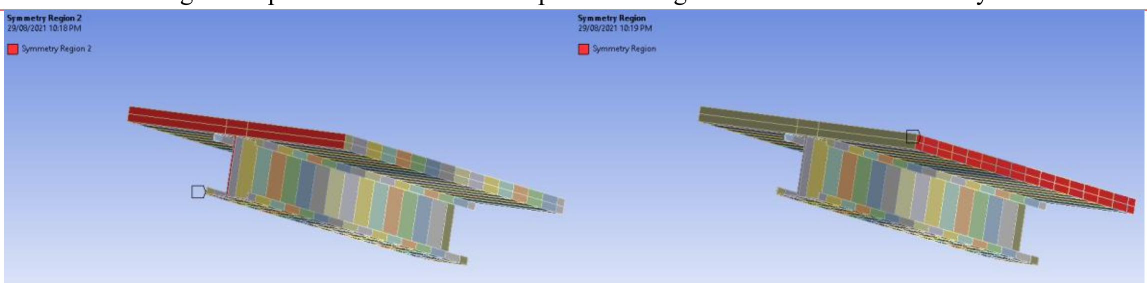

Fig. 8 Symmetry conditions applied on model

Table 5 summarises the results of the experimental testing carried out by Alhajri et al. (2016), and presents a comparison with the results of the current study. It can be observed that the finite element models developed in the current study determined the ultimate load and maximum deflection with over 95% accuracy. Therefore, the results of the numerical simulations conducted for the purposes of the current study have been found to closely agree with the four-point bending test results conducted by Alhajri et al. (2016).

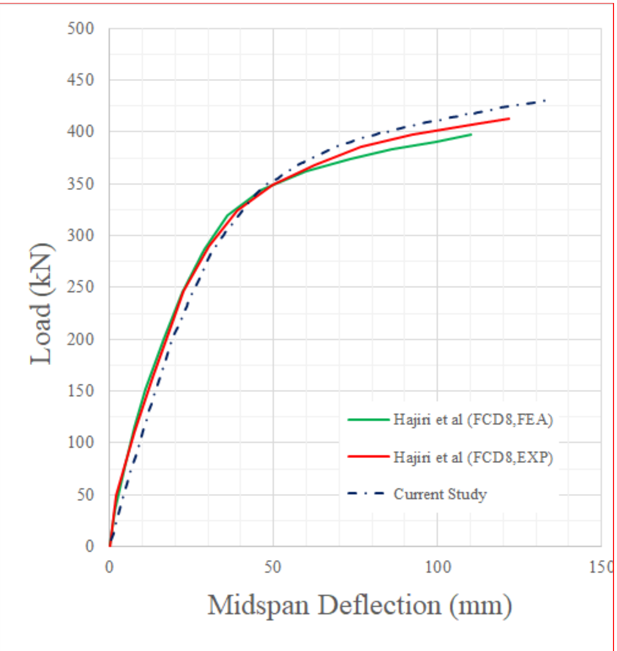

Fig. 11 Comparison of Load-deflection responses of Specimen FCD8.

Table 5 Summary of systems tested (adopted from Alhajri et al. 2016) for validation of numerical model

Specimen	FCD5	FCD8
Alhajri et al. (2016)'s Test Mu,exp (kN.m)	252.9	294.8
Current FEA Study Mu,FEA (kN.m)	253.7	307.7
MuFEA/Muexp	1.03	1.04

4. Parametric Studies and result discussion

Upon validation of the numerical model, the focus of the current investigation progressed to conducting a parametric study to evaluate the influence of different parameters on the load-deflection response of the proposed cold formed steel-reinforced concrete composite beam. This section describes the effect of implementing varying thicknesses of the concrete slab, varying thicknesses of the CFS beam, changing the spacing of the CFS beam, changing the spacing of the shear connectors (bolts), and utilising concretes of varying compressive strength. In all instances, the validated numerical model was used to investigate the influence of the various parameters. This model features reinforced concrete slab of thickness 50mm, CFS beams of thickness 3mm, spacing of CFS beams of 750mm, spacing of bolts of 150mm, and compressive strength of 35MPA. These dimensions and mechanical properties are identical to sample FCD5 as reported in Alhajri et al. (2016).

4.1 Thickness of concrete slab

In order to investigate the influence of the thickness of the reinforced concrete slab on the structural behaviour of the composite flooring system, the validated numerical model was used with mechanical properties as given in Tables 1, 2 and 3. For the purposes of the parametric study, three variations of the concrete thickness were used, 50mm, 60mm and 70mm. It can be seen from Fig. 12 that the

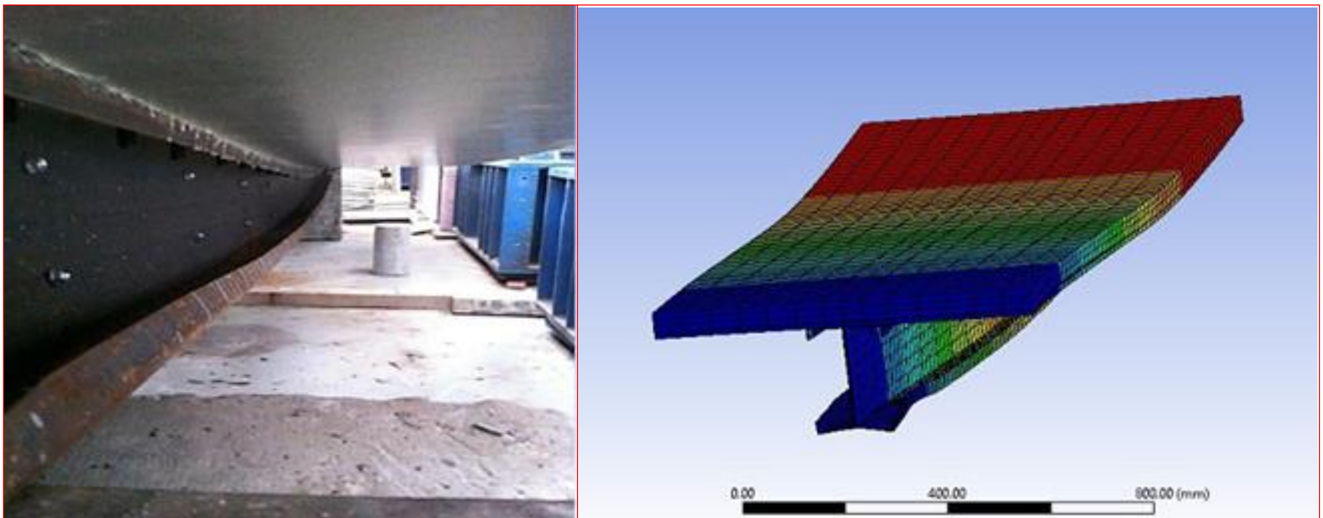

(a) Experimentally (Alhajri et al. 2016) (b) Current Study (FEA)

Fig. 9 Typical failure modes observed experimentally in Alhajri et al. (2016), and current Study (FEA) ultimate load increased from 362kN for the 50mm thick slab to 456kN and 506kN for the 60mm and 70m thick variations, respectively. This corresponds to moment capacity of 253, 319 and 254 kN.m, respectively. The stiffness (under service load) of the composite beam, which is the slope of the load-deflection curve of the composite beam (Karki, Far & Saleh 2021; Wong 2009) likewise increased with respect to the 50mm slab thickness by 38% and 48%, respectively. These results are summarised in Table 6.

The results show that increasing the thickness of the concrete slab yields a significant increase in moment capacity and stiffness. Load capacity likewise increased by 26% upon increasing slab thickness from 50 to 60mm, and by a further 11% upon increasing the slab thickness from 60mm to 70mm. This can be compared to an increase in volume of concrete of 20% and 17% for the two cases, respectively. The results show that increasing the slab thickness is a viable and economic option for increasing the capacity, and indicates that the 60mm slab thickness is the optimum thickness for optimising load capacity while minimising cost. The results also show that in applications requiring higher load capacity, such as storage as industrial facilitates, increased load capacity can be achieved by increasing the thickness of the concrete slab component of the composite flooring system.

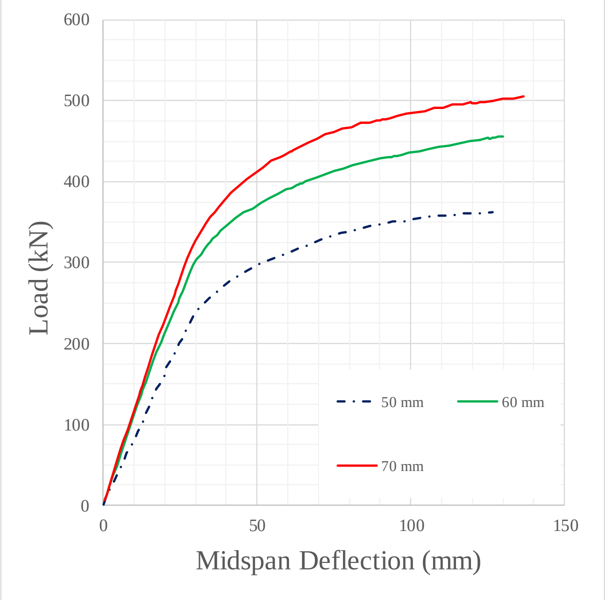

Fig. 12 Load and mid-span deflection curve of the composite CFS beam with different reinforced concrete slab thickness

Table 6 Determined moment capacity and stiffness of composite beams with different concrete slab thickness

Thickness of concrete slab	50mm	60mm	70mm
Ultimate load (kN)	362	456	506
Determined ultimate moment capacity (kN.m)	253	319	354
Mid-span deflection at ultimate load (mm)	127	130	137
Stiffness (kN/mm) under service load	7.94	11	11.8

4.2 Thickness of CFS beam

Three variations of CFS beam thickness were utilised to investigate the effect of this property on the load capacity and stiffness of the composite beam as shown in Figure 13. It is evident that increasing the thickness of the CFS beam to 4mm resulted in an increase in ultimate load capacity of 25%, and increased stiffness of 19%. However, reducing the CFS beam thickness to 2mm resulted in a decrease in the ultimate load capacity of 20% with minimal change in stiffness. The determined moment capacity for the 2, 3 and 4mmm thick CFS beam composite systems were 202, 253 and 302 kN.m, respectively. These results have been summarised in Table 7.

Table 7 Determined moment capacity and stiffness of composite beams with different CFS beam thickness

Thickness of CFS beam	2mm	3mm	4mm
Ultimate load (kN)	288	362	431
Determined ultimate moment capacity (kN.m)	202	253	302
Mid-span deflection at ultimate load (mm)	123	127	135
Stiffness (kN/mm) under service load	7.72	7.94	9.2

The results affirm the significant influence of CFS beam thickness on the load capacity and ultimate moment capacity of the composite system. This can be attributed to the increased second moment of inertia and section modulus resulting from increasing the thickness of the CFS beam. Fig. 13 further shows a variation in load deflection response and failure mode, such that the 2mm thick CFS beam exhibits a lower yield load compared to the 3 and 4mm thick CFS beams. Further, the load-deflection response of the 2mm specimen starts by an initial portion which is linear elastic, followed by deflection-softening, unlike the 3 and 4mm cases which maintain a positive, although decreasing stiffness, which is indicative of the earlier onset of flange buckling as shown in Fig. 14.

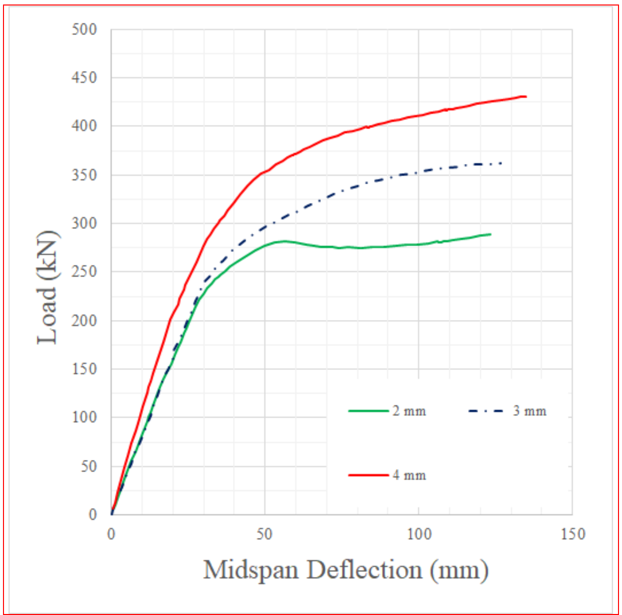

Fig. 13 Load and mid-span deflection curve of the composite CFS beam with different with different CFS beam thickness

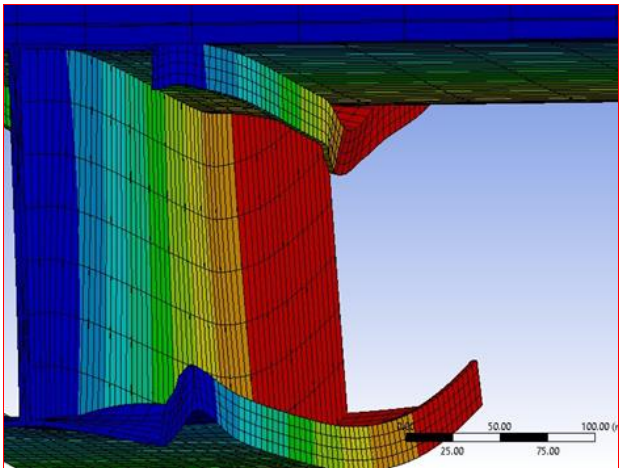

Fig. 14 Typical failure mode of composite beam with 2mm thick CFS beam observed in current study

4.3 Spacing of CFS beam

In order to investigate the influence of the spacing of the CFS beams, three variations of this dimension were analysed, each specimen otherwise identical dimensions. The variations analysed were 500mm, 750mm and 1000mm as shown in Fig. 15.

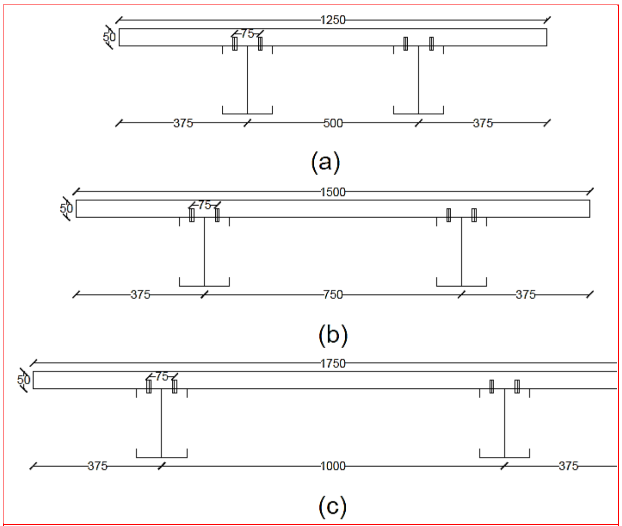

Fig. 15 Cross-section of cold-formed steel and reinforced concrete composite beam (a) 500mm spaced beams; (b) 750mm spaced beams; (c) 1000mm spaced beams

Fig. 16 shows that specimen c with beam spacing of 1000mm has the highest ultimate strength and stiffness, followed by specimens b (750mm) and a (500mm), respectively. This order is intuitive, as the 1000mm wide composite beam has the highest second moment of inertia and section modulus, followed by the 750mm and 500mm wide composite beams, respectively.

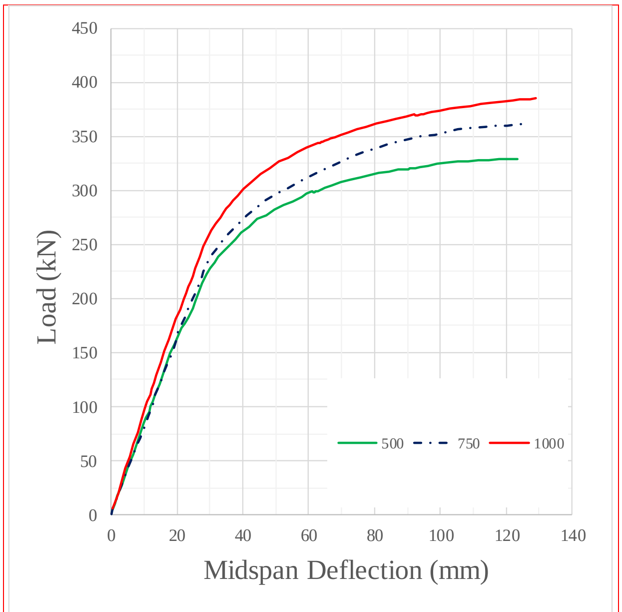

Fig. 16 Load and mid-span deflection curve of the composite CFS beam with different CFS beam spacing

The results are summarised in Table 8, showing an increase in ultimate load capacity, ultimate moment capacity and stiffness under service loading with increased beam spacing.

Table 8 Determined moment capacity and stiffness of composite beams with different Spacing of CFS beams

Spacing of CFS beam	500mm	750mm	1000mm
Ultimate load (kN)	330	362	380
Determined ultimate moment capacity (kN.m)	231	253	266
Mid-span deflection at ultimate load (mm)	124	127	129
Stiffness (kN/mm) under service load	7.72	7.94	8.89

Increasing the spacing of the CFS has effectively increased the dimensions of the composite beam specimen, increasing the area above the neutral axis, increasing the second moment of area and section modulus and thereby making the beam increasingly resistant to bending under loading. The increase in second moment of inertia and section modulus resulting from the increased spacing yields higher strength and stiffness of the composite system, as evidenced by the results summarized in Table 8. Notably, the ultimate moment capacity of the composite flooring system increased by 7% upon increasing spacing from 750mm, which is the spacing implemented in the benchmark study by (Alhajri et al. 2016), to 1000mm. Conversely, reducing the spacing from 750mm to 500mm yields a 10% decrease in moment capacity. The stiffness of the composite beam increased by 2.8% and 11% upon increasing spacing of beams from 500mm to 750mm, and from 750mm to 1000mm, respectively.

The disparities in moment capacity can be contrasted to the self-weight of the floor. From Table 9 it can be observed that the beam spacing of 750mm provides the best strength to weight ratio. In principal, this implies this option would provide the most cost-efficient option out of the three alternatives, However, in designing a similar floor system, other requirements need to be considered, including serviceability requirements, particularly with regards to excessive floor vibration (Zhang 2017) and constructability issues such the requirement to run services such as air ducts, pipes and electric fixtures through the CFS beams.

Table 9 Determined Moment Capacity to Weight Ratio of composite beams with different Spacing of CFS beams

Spacing of CFS beams	Self-weight of floor	Estimated Moment Capacity (kN.m)	Moment Capacity to Weight Ratio
500	173.8	166	0.955
750	208.1	253	1.22
1000	278.1	270	0.971

4.4 Spacing of bolts

The effect of the bolt spacing was investigated by analysing composite beams with three different bolt spacing configurations. These variations were 75mm, 150mm as in the 4 point bending test carried out by Alhajri et al. (2016), and 300mm. The load and mid-span deflection response of the three variations are shown in Fig. 17.

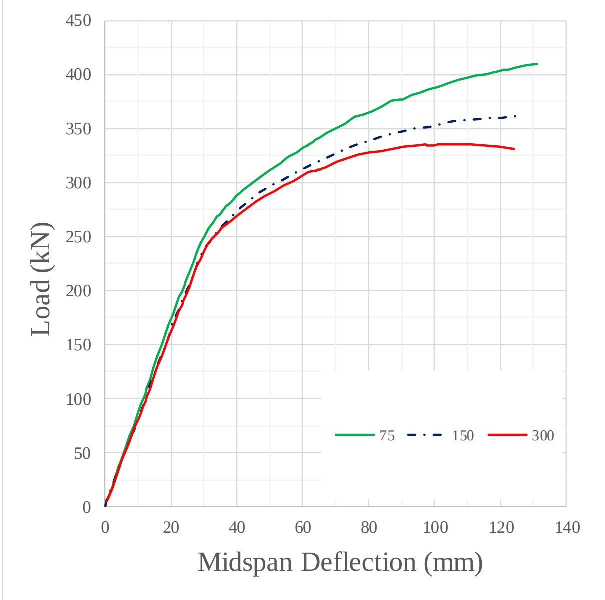

Fig. 17 Load and mid-span deflection curve of the composite CFS beam with different bolt spacing (mm)

The determined ultimate load, ultimate moment capacity and stiffness of the composite beams with the three variations of bolt spacing are shown in Table 10. It is apparent that the ultimate moment capacity of the composite beam increased by 9% and 13% as the bolt spacing was reduced from 300mm to 150mm, and from 150mm to 75mm, respectively.

Table 10 Determined moment capacity and stiffness of composite beams with different bolt spacing

Bolt Spacing	75mm	150mm	300mm
Ultimate load (kN)	410	362	331
Determined ultimate moment capacity (kN.m)	287	253	232
Mid-span deflection at ultimate load (mm)	131	127	124
Stiffness (kN/mm) under service load	8.1	7.94	7.62

The results show the significant effect of bolt spacing on the load capacity of the composite beam. Reduced bolt spacing results in an increase in the mobilisation of composite action between the CFS beam and the concrete slab, as previous research has shown (Bamaga et al. 2013; Far 2020). This Increased mobilisation enhances composite action between the CFS beam and concrete slab, as well as reducing the length of the of the CFS beam between bolts, reducing the occurrence of local buckling between the shear connectors. In the case of the 300mm bolt spacing, increased spacing led to insufficient restraint to the flange of the CFS and hastened the onset of local buckling.

4.5 Compressive strength of reinforced concrete.

The validated numerical model was utilised to investigate the effect of concrete grade (compressive strength) on the ultimate strength of the composite flooring system. Five grades of concrete were considered, C35, C40, C50, C60, and C70. These variations include concrete grades typically used in Australia as per AS 3600 (Standards Australia 2018) . As expected, stiffness and ultimate strength of the composite beams were both influenced by concrete grade, as illustrated in Fig. 18.

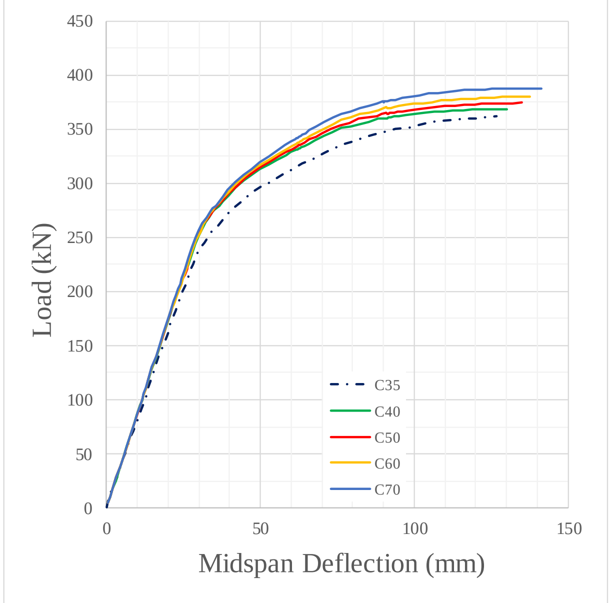

Fig. 18 Load and mid-span deflection curve of the composite CFS beam with different concrete grades

The determined moments capacities of the composite flooring system featuring the various concrete grades are tabulated in Table 11.

Table 11 Determined moment capacity and stiffness of composite beams with different concrete grade

Concrete Grade	35 MPa	40 MPa	50 MPa	60 MPa	70 MPa
Modulus of Elasticity E	26200	30334	33915	34845	36507
Ultimate load (kN)	362	369	374	380	388
Determined ultimate moment capacity (kN.m)	253	258	262	266	272
Mid-span deflection at ultimate load (mm)	127	130	135	138	141
Stiffness (kN/mm) under service load	7.94	8.38	8.46	8.47	8.64

The results show the ultimate load, ultimate moment and stiffness increase with each increase in concrete grade, while maintaining ductility. This result shows that increasing the concrete strength can lead to higher overall beam strength. The composite beam typically failed due to buckling of the CFS beam. This indicates that further mobilisation of composite action, possibly though the enhancement of the shear connection, may further increase the ultimate capacity of the composite beam, noting that all cases represented in Figure 18 had 150mm bolt spacing. It should be noted that enhanced resistance of the shear connectors due to increase in compressive strength of concrete has been conservatively neglected, in accordance with section 3.6.2.3 of AS/NZS 2327 (Standards Australia 2017). Future research will be aimed at identifying and harnessing any potential enhancement in shear connection when employing higher concrete grades.

The results also indicate the composite beam can work well with lower grade concrete, while still achieving good overall ultimate strength, therefore reducing the cost. This aspect further suggests the suitability of using geopolymer concretes, which possess lower early strength than comparable Ordinary Portland Cement based-concretes (Deb, Nath & Sarker 2015), for use in the proposed composite flooring system.

4.5 Global optimisation of composite beam.

The validated numerical model was utilised to investigate the effect of selecting the optimum design parameters obtained in sections 4.1 to 4.4, and creating a globally optimised composite beam based on these parameters. Accordingly, a comparison of the loading capacity of the globally optimised composite beam with the original beam (specimen FCD5, Table 4 and Fig. 10) can be carried out. The results of this exercise are given in Figure 19 and Table 12.

Table 12 Determined moment capacity and stiffness of the globally optimised composite beam

Specimen	FCD5	Globally optimized composite beam
CFS beam thickness (mm)	3	4
Bolt spacing (mm)	150	75
Thickness of reinforced concrete slab (mm)	50	70
CFS beam spacing (mm)	750	500
Concrete grade (MPa)	35	70
Ultimate load (kN)	362	490
Determined ultimate moment capacity (kN.m)	253	350
Mid-span deflection at ultimate load (mm)	127	141
Stiffness (kN/mm) under service load	7.94	9.72

Source: Adapted from Alhajri et al. (2016)

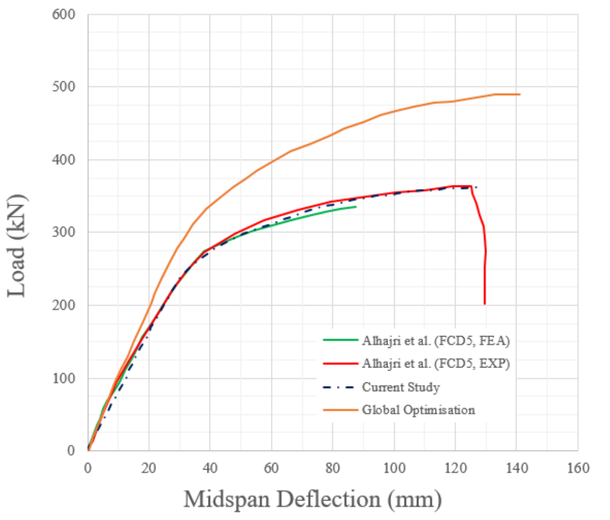

Fig. 19 Comparison of Load-deflection responses of Specimen FCD5 with globally optimised composite beam

The results presented in Table 12 and Figure 19 show that upon implementing the optimised design parameters, it is apparent that the ultimate moment capacity of the composite beam increased by 38% while mid-span deflection at ultimate load and stiffness under service load have also increased significantly. Distortional buckling was observed in the bottom flange of the CFS beam as shown Fig. 20. These results endorse and extend the findings of sections 4.1 to 4.4, confirming that increasing the thickness of the reinforced concrete slab, the thickness of the cold formed steel (CFS) beams, and the concrete grade while reducing the spacing of bolts and spacing of the CFS also lead to an increase in determined ultimate moment capacity and overall enhanced structural performance of the composite beam.

5. Conclusions

This paper reports the findings of a numerical investigation of the structural performance of a composite reinforced concrete-cold formed steel (CFS) beam. A Finite Element Model was developed and validated against experimental results, stemming from four-point bending tests conducted by Alhajri et al. (2016).

Utilising the validated numerical model, a parametric study was performed with the aim of determining the effect of various parameters on the flexural behaviour of the composite system. These parameters were thickness of the concrete slab, thickness of the CFS beam, spacing of bolts, spacing of the beams and concrete grade.

The investigation of the effect of the concrete slab thickness showed that increasing this value resulted in an increase in ultimate load capacity and stiffness of the composite system. The thickness of the CFS beam was found to have significant effect on the mechanical properties of the composite flooring system, with results showing an increase in ultimate moment capacity and stiffness with increased CFS thickness. Reduction of the spacing of shear connectors was found to result in increased ultimate strength, as results showed reducing the bolt spacing from 300mm to 150mm and from 150 to 75mm, resulted in an improvement in ultimate moment capacity of 9% and 13%, respectively.

The results also showed that increasing the spacing of the CFS beams from 500mm to 750mm produced an increase in ultimate moment capacity of 10%. The 750mm CFS beam spacing was also found to produce the highest ultimate moment capacity to weight ratio, indicating the economic benefits of using this configuration.

Increasing the concrete grade from the benchmark 35C (compressive strength of 35 MPa) to 40, 50, 60 and 70MPa resulted in increased moment capacity, ultimate load and stiffness. As the failure of the composite beam typically occurred due to buckling of the CFS beam, further mobilisation of composite action could result in better utilisation of the concrete slab and there achieving higher ultimate moment capacity. Provisions of international codes including AS/NZS 2327 refer to the relation between the capacity of the shear connectors and the strength of the concrete. Future research shall include push out tests to identify the specific load-slip behaviour of each concrete grade used in the current study. These results can be further utilised to update the numerical model.

The results of the current research provide useful findings for the design of an efficient flooring system, with optimised mechanical properties including strength and stiffness, which can be achieved by design a composite floor with suitable concrete thickness, CFS beam thickness, shear connector spacing, beam spacing and concrete grade. Optimisation of these parameters enables the construction of an efficient, lightweight and cost-effective flooring system which can be tailored to various uses and applications.

Acknowledgments

This research is supported by an Australian Government Research Training Program (RTP) Scholarship.

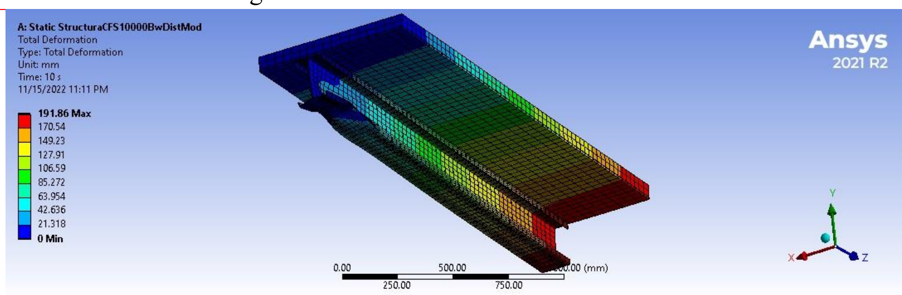

Fig. 20 Failure mode of globally optimised composite beam

References

Abdel-Sayed, G. 1982, 'Composite Cold-formed Steel-concrete Structural System', *6th International Specialty Conference onCold-Formed Steel Structures*, <https://scholarsmine.mst.edu/isccss/6iccfss/6iccfss-session9/2>.

Ahmed, I.M. & Tsavdaridis, K.D. 2019, 'The evolution of composite flooring systems: applications, testing, modelling and eurocode design approaches', *Journal of Constructional Steel Research*, vol. 155, pp. 286-300, <https://doi.org/10.1016/j.jcsr.2019.01.007>.

Alhajri, T.M., Tahir, M.M., Azimi, M., Mirza, J., Lawan, M.M., Alenezi, K.K. & Ragaee, M.B. 2016, 'Behavior of pre-cast U-Shaped Composite Beam integrating cold-formed steel with ferro-cement slab', *Thin-Walled Structures*, vol. 102, pp. 18-29, <https://doi.org/10.1016/j.tws.2016.01.014>.

ANSYS Inc. 2021, *ANSYS 2021 R2*, ANSYS, Inc., Canonsburg, Pennsylvania.

Bamaga, S.O., Tahir, M.M., Tan, C.S., Shek, P.N. & Aghlara, R. 2019, 'Push-out tests on three innovative shear connectors for composite cold-formed steel concrete beams', *Construction and Building Materials*, vol. 223, pp. 288-98, <https://doi.org/10.1016/j.conbuildmat.2019.06.223>.

Bamaga, S.O., Tahir, M.M., Tan, T.C., Mohammad, S., Yahya, N., Saleh, A.L., Mustaffar, M., Osman, M.H. & Rahman, A.B.A. 2013, 'Feasibility of developing composite action between concrete and cold-formed steel beam', *Journal of Central South University*, vol. 20, no. 12, pp. 3689-96, <10.1007/s11771-013-1897-9>.

BSI 2005, *BS EN 1994-1-1:2004 Eurocode 4. Design of composite steel and concrete structures. General rules and rules for buildings*, British Standards Institute,, London.

Deb, P., Nath, P. & Sarker, P. 2015, 'Drying Shrinkage of slag blended fly ash geopolymer concrete cured at room temperature', <10.1016/j.proeng.2015.11.066>.

Far, H. 2020, 'Flexural Behavior of Cold-Formed Steel-Timber Composite Flooring Systems', *Journal of Structural Engineering*, vol. 146, no. 5, p. 06020003, <10.1061/(ASCE)ST.1943-541X.0002600>.

Framecad 2018, 'US Navy Explores Cold Fromed Steel Framing', 05/11/2018, viewed 22/10/2020, <https://www.framecad.com/en/construction/customer-stories/us-navy-explores-cold-formed-steel-framing/>.

Grand View Research 2021, *Light Gauge Steel Framing Market Size, Share & Trends Analysis Report by Type (Long Span, Wall Bearing, Skeleton), by End-use (Commercial, Residential), by Region (APAC, North America), and Segment Forecasts, 2021-2028*, Grand View Research;, San Francisco, USA.

Hanaor, A. 2000, 'Tests of composite beams with cold-formed sections', *Journal of Constructional Steel Research*, vol. 54, no. 2, pp. 245-64, <https://doi.org/10.1016/S0143-974X(99)00046-2>.

Hosseinpour, M., Zeynalian, M., Ataei, A. & Daei, M. 2021, 'Push-out tests on bolted shear connectors in composite cold-formed steel beams', *Thin-Walled Structures*, vol. 164, p. 107831, <https://doi.org/10.1016/j.tws.2021.107831>.

Irwan, J.M., Hanizah, A.H., Azmi, I. & Koh, H.B. 2011, 'Large-scale test of symmetric cold-formed steel (CFS)–concrete composite beams with BTTST enhancement', *Journal of Constructional Steel Research*, vol. 67, no. 4, pp. 720-6, <10.1016/j.jcsr.2010.11.008>.

Karki, D., Far, H. & Saleh, A. 2021, 'Numerical studies into factors affecting structural behaviour of composite cold-formed steel and timber flooring systems', *Journal of Building Engineering*, vol. 44, p. 102692, <https://doi.org/10.1016/j.jobe.2021.102692>.

Kyvelou, P. 2017, 'Structural Behaviour of Composite Cold-Formed Steel Systems', Imperial College London.

Kyvelou, P., Gardner, L. & Nethercot, D.A. 2018, 'Finite element modelling of composite cold-formed steel flooring systems', *Engineering Structures*, vol. 158, pp. 28-42, <10.1016/j.engstruct.2017.12.024>.

Lakkavalli, B.S. & Liu, Y. 2006, 'Experimental study of composite cold-formed steel C-section floor joists', *Journal of Constructional Steel Research*, vol. 62, no. 10, pp. 995-1006, <10.1016/j.jcsr.2006.02.003>.

Malite, M., Nimir, W.A., Sales, J.J.d. & Goncalves, R.M. 1998, 'Cold-formed Shear Connectors for Composite Constructions', *14th International Specialty Conference on Cold-Formed Steel Structures*, Missouri University of Science and Technology, <https://scholarsmine.mst.edu/isccss/14iccfsss/14iccfsss-session7/2>.

Mantha, A. 2014, 'Analytical Evaluation of Inorganic Polymer Materials for Infrastructure Repair ', Rutgers, The State University of New Jersey, New Brunswick, USA.

Nakamura, S.-i. 2002, 'Bending Behavior of Composite Girders with Cold Formed Steel U Section', *Journal of Structural Engineering*, vol. 128, no. 9, pp. 1169-76, <doi:10.1061/(ASCE)0733-9445(2002)128:9(1169)>.

Nguyen, R.P. 1991, 'Thin-Walled, Cold-Formed Steel Composite Beams', *Journal of Structural Engineering*, vol. 117, no. 10, pp. 2936-52, <10.1061/(ASCE)0733-9445(1991)117:10(2936)>.

Paton-Cole, V. & Gad, E. 2017, *Understanding the Benefits of Constructing a Residential House with a Heart of Cold-Formed Steel*.

Rasmussen, K.J.R., Khezri, M., Schafer, B.W. & Zhang, H. 2020, 'The mechanics of built-up cold-formed steel members', *Thin-Walled Structures*, vol. 154, p. 106756, <https://doi.org/10.1016/j.tws.2020.106756>.

Standards Australia 2017, *Composite structures - Composite steel-concrete construction in buildings*, Standards Australia, Sydney.

Standards Australia 2018, 'AS 3600:2018 Concrete Structures',

Wehbe, N., Wehbe, A., Dayton, L. & Sigl, A. 2011, 'Development of Concrete/Cold Formed Steel Composite Flexural Members', *Structures Congress 2011*, pp. 3099-109.

Wills, R.J. 2015, 'Cold-formed steel design standards', *The Construction Specifier*,

Wong, M.B. 2009, 'Chapter 2 - Plastic Behavior of Structures', in M.B. Wong (ed.), *Plastic Analysis and Design of Steel Structures*, Butterworth-Heinemann, Boston, pp. 55-80.

Yu, W.-W., LaBoube, R.A. & Chen, H. 2020, *Cold-Formed Steel Design*, 5 edn, John Wiley & Sons, Inc.

Zhang, S. 2017, 'Vibration Serviceability of Cold-Formed Steel Floor Systems', University of Waterloo, Waterloo, Ontario, Canada.